Preparation, Characterization, and Surface Modification of Silver Nanoparticles in Formamide

Anjana Sarkar, Sudhir Kapoor,* and Tulsi Mukherjee

Radiation Chemistry & Chemical Dynamics Division, Bhabha Atomic Research Centre, Mumbai 400 085, India

Received: December 21, 2004; In Final Form: February 21, 2005

The reduction of silver ions in formamide is shown to take place spontaneously at room temperature without addition of any reductant. The growth of Ag particles was found to be dependent on Ag^+ ion concentration. In the absence of any stabilizer, deposition of silver film on the glass walls of the container takes place. However, in the presence of poly(*N*-vinyl-2-pyrrolidone) (PVP) or colloidal silica (SiO_2), which are capable of stabilizing silver nanoparticles by complexing and providing support, a clear dispersion was obtained. The formation of the silver nanoparticles under different conditions was investigated through UV−visible absorption spectrophotometry, gas chromatography, and also electron and atomic force microscopic techniques. Atomic force microscopy results for silver films prepared in the absence of any stabilizer showed the formation of polygonal particles with sizes around 100 nm. Transmission electron microscopy results showed that the prepared silver particles in the presence of PVP were around 20 nm. The Ag nanoparticles get oxidized in the presence of chloroform and toluene. Surface modification of silver film was done in the presence of the tetrasodium salt of ethylenediaminetetraaceticacid (Na_4EDTA). It was shown that the reactivity of the silver film increased in its presence. The Fermi potential of silver particles in the presence of Na_4EDTA seems to lie between −0.33 and −0.446 V vs NHE.

Introduction

A large number of methods have been developed for the synthesis of metal nanoparticles since the discovery by Faraday on metal particles.[1] To stabilize metal nanoparticles, generally synthetic polymers[2−6] and ligands[7−13] are widely used. Such substances can also control the reduction rate of metal ions and the aggregation processes of the metal clusters.[3−11] The interaction of polymer with metal ions plays a crucial role in controlling the size and morphology of the particles. El-Sayed et al.[12] have shown that, by changing the capping ratio of metal ions to polymer, one can control the shape of the nanoparticles.

Recently, metals or semiconductor nanoparticles synthesized by various techniques have found potential application in many fields such as catalysis, sensors, etc.[14−17] In most of the applications, nanoparticles are used as building blocks toward functional nanostructures. The coinage metal nanoparticles such as silver, gold, and copper are mostly exploited for such purposes as they have surface plasmon resonance absorption in the UV−visible region.[3] The surface plasmon band arises from the coherent existence of free electrons in the conduction band due to the small particles size effect, which is dependent on the particle sizes, chemical surrounding, adsorbed species on the surface, and dielectric constant.[3−6] The unique feature of the coinage metal nanoparticles is that a change in the absorbance or wavelength provides a measure of the particle size, shape, and interparticle properties. In this, one-dimensional nanostructures such as wires, rods, etc. have become the focus of intensive research because of their unique applications.[14−17] For small particles (<2 nm), the surface plasmon band is strongly damped due to low electron density in the conduction band. However, as particle size increases, the intensity of the surface plasmon band increases. It has been suggested that, although both absorbance and scattering contribute to the optical property, the contribution of the latter is relatively insignificant as compared to that of the former for very small nanoparticles (≤15 nm).[14−23]

Recently, Liz-Marzan et al.[24−28] have shown that silver nanoparticles can be prepared in DMF without adding any reductant. It has been suggested that the reduction rate can be enhanced at high temperatures. Because most of the organic reactions take place in organic solvents, it is desirable to develop synthetic methods that lead to the formation of particles having different morphology in addition to the stabilization of metal nanoparticles in such solvents. In addition, if one can design a synthetic method to prepare different morphological particles in the same medium without adding reductants from outside, this may have its own important implications.

Formamide is one of the most common solvents used to study various processes such as formation of metal nanoparticles, interaction with alcohols, etc.[29−32] It is known that formamide−water and formamide−methanol complexes can serve as model systems for protein−water and protein−solvent interactions. Photocatalytic oxidation of volatile organic chemicals (VOCs) constitutes one of the most promising methods for the removal of these pollutants in an enclosed atmosphere.[33−35] Generally, metal oxides are being explored for such purposes.[33,34] As silver is known to have bactericidal properties, it is important to assess its effect on VOCs. In this paper, we describe in detail the preparation of silver nanoparticles by reduction of silver ions with formamide in the absence and presence of stabilizers such as poly(*N*-vinyl-2-pyrrolidone) (PVP) and SiO_2 nanoparticles. In addition, attempts have been made to see the effect of addition of methanol, VOCs, and a complexing agent on the stability of silver nanoparticles.

* Corresponding author. Tel.: (+)91-22-25590298. Fax: (+)91-22-25505151. E-mail: sudhirk@apsara.barc.ernet.in.

10.1021/jp044201r CCC: $30.25
Published on Web 03/30/2005

Experimental Section

Materials. Silver perchlorate (Aldrich), $AgNO_3$ (BDH, India), tetrasodium salt of ethylenediaminetetraaceticacid (Sigma), methanol, $CHCl_3$ and toluene (UV spectroscopy grade, Spectrochem, India,), PVP (mol wt. = 360 000 and 40 000) (Sigma), methyl viologen dichloride {paraquat: 1,1′-dimethyl 4,4′-dipyridinium dichloride; MV^{2+} $(Cl^-)_2$} (Aldrich), and SiO_2 (LUDOX SM-30, Aldrich) were used as received. IOLAR grade N_2 gas (purity ≥99.99%) used for purging solutions was obtained from Indian Oxygen Limited. All solutions were prepared just before the experiments and kept in dark to avoid any photochemical reactions. Water purified through a Millipore system was used.

Film Preparation. The slides were cleaned in perchloric acid. After being rinsed with distilled and Millipore water, they were dried in an oven. The slides were suspended in formamide solution containing varying concentrations of silver ions. Film formation takes place with time on the surface of the slide. The slides were removed after 24 h and dried at room temperature. Care was taken to protect these slides from light both during and after film formation.

Preparation of Silver Nanoparticles in the Presence of Stabilizer. Dispersions of silver nanoparticles were prepared by mixing the required concentration of PVP or SiO_2 in formamide followed by addition of silver salt at room temperature. With time, the solution gradually turned yellow, and evolution of a stable dispersion of silver nanoparticles was observed.

Charge and Size Determination. Zeta potential measurements, for determining the size and charge on SiO_2 nanoparticles in formamide and water, were carried out using Malvern Instrument, zeta sizer (nanosizer). No sign of agglomeration and/or precipitation of SiO_2 nanoparticles in formamide was found at least up to 45 days.

Gas Chromatography Experiments. Silver dispersions were prepared in rectangular quartz cells of dimension 1 cm × 1 cm × 5 cm. The solution was bubbled with nitrogen, and the cell was closed with a self-sealing septum. The evolved gas was measured using a gas chromatograph after 28 h. For CO_2 detection, a Porapak Q-S column and a thermal conductivity detector were used. Helium was used as a carrier gas. Attempt was also made to see the evolution of other gases, if any. For H_2 detection, a column with molecular sieve-5A and N_2 as carrier gas was used. The temperatures of the measurements for CO_2 and H_2 were 40 and 32 °C, respectively.

Amount of Silver Metal Formed. The amount of silver metal formed during the reduction of silver ions was determined after 28 h using a Chemito AA203 atomic absorption spectrophotometer (AAS). The slit width and lamp current were 0.5 nm and 5 mA, respectively. The silver was detected at 228 nm using an air acetylene flame.

Characterization. Samples for transmission electron microscopy (TEM) were prepared by putting a drop of the colloidal solution on a copper grid coated with a thin amorphous carbon film. Samples were dried and kept under vacuum in a desiccator before being put in a specimen holder. TEM characterization was carried out using a JEOL JEM-2000FX electron microscope. Particle sizes were measured from the TEM micrographs and calculated by taking at least 100 particles. Absorption measurements were carried out on a JascoV-530 spectrophotometer. The spectra were recorded at room temperature using either a 0.2 or a 1 cm quartz cuvette. However, all of the spectra were later normalized to 1 cm path length of the cuvette. Atomic force microscopy (AFM) characterization was carried out using a Solver P-47H microscope. AFM measurements were done by contact mode using Si_3N_4 tip, the resonance frequency and spring constant being 100 kHz and 0.6 N/m, respectively.

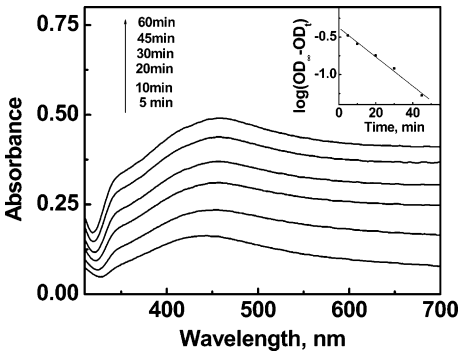

Figure 1. Time-dependent UV−visible absorption spectra of silver nanoparticles in formamide. Inset: First-order kinetics for the formation of silver nanoparticles in formamide.

Dynamic light scattering experiments were done on a Malvern 4800 Autosizer employing a 7132 digital correlator. The intensity correlation function was analyzed by method of cumulants using the mean and variance of the distribution on the fitted variable. The diffusion coefficient (D) of the particle is related to the average decay rate (Γ) of the correlation function by $\Gamma = Dq^2$, where q is the magnitude of the scattering vector (given by $q = 4\pi n/\lambda \sin \theta/2$; λ is the wavelength of light, n is the refractive index, and q is the scattering angle). The mean hydrodynamic coefficient of the particles was obtained from the diffusion coefficient using the Stokes−Einstein relationship. The light source was an Ar^+ ion laser operated at 514.5 nm and a scattering angle $q = 90°$.

Results and Discussion

Reduction of Silver Ions. On addition of silver salt to neat formamide in the absence of any stabilizer, the color of the solution changed from yellow to gray. As the reaction proceeded, deposition of silver film started on the glass walls of the vessel within a few hours while the solution turned transparent. This clearly indicates that silver particles are first formed in the solution and then deposited on the walls of the container. The color of the film was found to depend on the concentration of the silver salt and varied from yellow to brown. However, if the solution was left in the vessel for more than 24 h, then metallic shining silver particles were found to attach onto the glass walls of the container. This process is probably driven by electrostatic attraction between the particles having positive charge due to the adsorption of unreacted silver ions and the negatively charged SiO_2 surface. The rate for the growth of Ag particles was found to depend on the concentration of silver ions. A typical variation of absorbance with time for 5×10^{-3} mol dm^{-3} silver nitrate solution in formamide is shown in Figure 1. The kinetics for the evolution of the absorption band was measured at 450 nm with time (inset Figure 1). The rate constant for the evolution of silver particles was found to be 0.046 min^{-1}.

With time, evolution of gas was observed on addition of silver salt in formamide. Several routes are possible for the oxidation of formamide, and the process may involve the evolution of NH_3, CO_2, and H_2 gases.[36] To know the gases evolved during the reaction as well as to understand the reduction process clearly, gas-chromatographic experiments were carried out. The evolved gas after a constant time (28 h) was measured using a gas chromatograph, for solutions containing silver dispersion

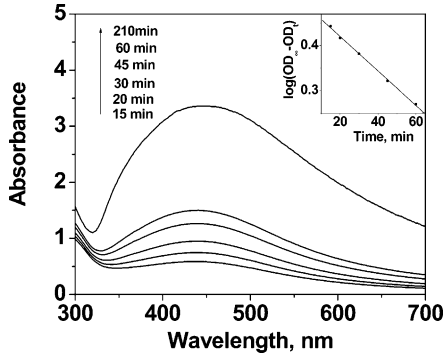

Figure 2. Time-dependent UV−visible absorption spectra of silver nanoparticles in formamide in the presence of 1.5 g/L SiO_2. Inset: First-order kinetics for the formation of silver nanoparticles in formamide in the presence of SiO_2.

and neat formamide. In solution containing silver dispersion, it was observed that the evolved gas was CO_2. The amount of CO_2 evolved was found to be 2.04 μmol for a solution containing 10^{-2} mol dm^{-3} Ag^+ in formamide. The amount of Ag metal formed was determined by AAS after an identical time (28 h) to quantify the amount of CO_2 evolved. The amount of CO_2 liberated was found to be 0.1059 mol and 2.4×10^{-5} mol per mol of Ag metal and formamide, respectively. It is important to mention here that CO_2 was not observed in absence of silver ions under identical conditions in neat formamide. It is pertinent to mention here that during reduction of silver ions by DMF evolution of CO_2 does not occur.[24−28] This shows that the reduction of silver ions in formamide and DMF follows different mechanisms.

Effect of Stabilizers and Counterion. When a stabilizing agent such as SiO_2 or PVP was added to formamide before addition of silver salt, stable clear dispersions of silver colloids were obtained. However, no adsorption of metallic silver on the walls of the container was observed in the presence of SiO_2 or PVP. Therefore, to restrict the size of the nanoparticles (or to get clear dispersions of Ag nanoparticles) and to study the evolution of silver nanoparticles, different methodologies were adopted. In the first case, silica nanoparticles (13 nm) were used to provide support for silver nanoparticles. Figure 2 shows the evolution of silver nanoparticles stabilized by SiO_2. On comparison with the results obtained in Figure 1, it can be noted that in the presence of silica the rate of formation of silver particles decreases drastically. For 1×10^{-2} mol dm^{-3} $AgNO_3$ solution containing 1.5 g/L of SiO_2, the rate constant for the evolution of the surface plasmon absorption band of silver particles was evaluated from the kinetic plot (inset Figure 2) and found to be 0.0086 min^{-1}. It is important to clarify here that the low absorbance yield in Figure 1 as compared to that obtained in Figure 2 is due to the fact that in absence of SiO_2 silver particles got deposited on the walls of the container.

The size of the nanoparticles at a particular ratio of Ag^+/SiO_2 was determined by dynamic light scattering. A representative case is shown in Figure 3. The particle size was around 38 nm for 1×10^{-2} mol dm^{-3} $AgNO_3$ solution containing 1.5 g/L SiO_2. The variation in the size of the particles with [Ag^+] keeping the amount of SiO_2 constant was also determined (Table 1). It can be noted that as the concentration of Ag^+ ions increased the size of the particles decreased. This can be explained by assuming that, to generate small and monodispersed particles, the nucleation and particle growth processes should occur on different time scales.[37] As the rate of evolution of silver particles increases with the concentration of silver ions,

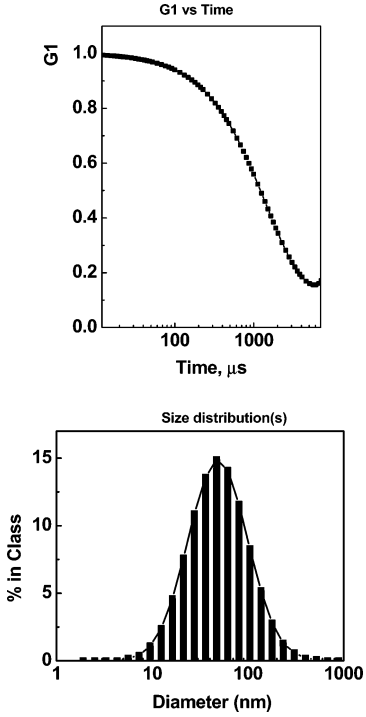

Figure 3. Dynamic light scattering results showing monodispersity and particle size distribution of silver nanoparticles prepared from 1×10^{-2} mol dm^{-3} $AgNO_3$ in formamide containing 1.5 g/L SiO_2.

TABLE 1: Effect of Silver Ion Concentration on the Size of Silver Nanoparticle Containing 1.5 g/L SiO_2

[Ag^+], mol dm^{-3}	diameter, nm
3×10^{-3}	48
1×10^{-2}	38

it appears that this could be the reason for observing smaller particles at higher concentration of Ag^+ ions.

To confirm the charge on colloidal SiO_2 in formamide, its zeta potential was determined. It was noted that the charge on colloidal SiO_2 in formamide becomes more negative (−56.7 mV) as compared to that in water (−37.3 mV). The zeta potential, ξ, of colloid particles is sensitive to the inverse Debye screening length (κ) of the medium, which in turn is decided by the ionic strength and dielectric constant of the medium. An increase in dielectric constant decreases the value of κ, thereby increasing the effective potential of the particle at the shear plane. This explains the observed increase in the charge of colloidal SiO_2 in formamide as compared to that in water. Due to negative charge on the surface of SiO_2 particles, the encounters between the particles are inhibited. This helps in stabilizing small Ag particles on its surface. The results obtained corroborate the earlier findings in aqueous solutions.[38,39]

Figure 4 shows the surface plasmon absorption band of silver nanoparticles obtained at different times in formamide containing 2×10^{-3} mol dm^{-3} $AgNO_3$ and 1% PVP (wt/v). The increase in the intensity of the surface plasmon band at around 425 nm indicates the continuous formation of silver particles. After an hour, the relative increase in the growth of the particles decreased as can be seen in Figure 4. It can be noticed that the surface plasmon absorbance band remains symmetric and no significant change in the width of the band with time was observed. This implies that the size of the nanoparticles remains more or less uniform. The surface plasmon absorption band position of silver particles in formamide in the presence of PVP was centered at 425 nm, which was red shifted with respect to the absorption maximum of silver particles prepared in an

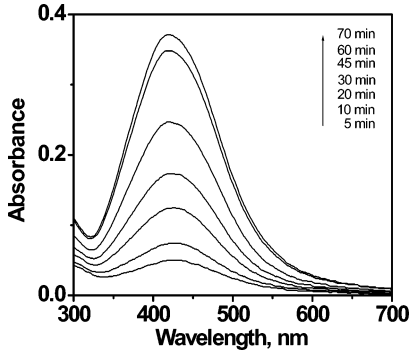

Figure 4. Time-dependent UV−visible absorption spectra of silver nanoparticles obtained from reduction of 2×10^{-3} mol dm^{-3} $AgNO_3$ in formamide containing 1% PVP (wt/v).

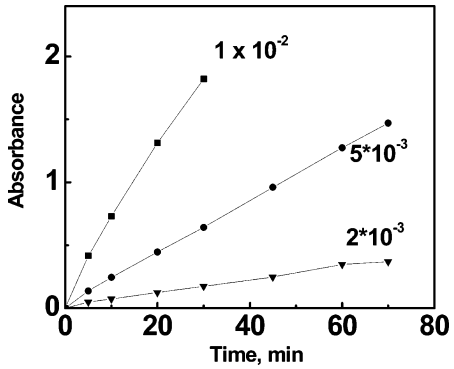

Figure 5. Kinetic traces for the formation of silver nanoparticles in formamide with increase in the concentration of silver ion keeping PVP concentration constant (1 wt %/v).

aqueous solution. The possible reason for this is the higher refractive index of formamide as compared to that of water. This is in agreement with the prediction by Mie theory. Kinetic traces showing formation of silver particles in formamide for different Ag^+ concentrations in the presence of constant PVP (1.0 wt %/v) are shown in Figure 5. It can be seen from the figure that the rate of evolution of particles increases with an increase in silver ion concentration. Similar results were obtained when PVP of low molecular weight (40 000) was used. It should be mentioned here that we could not observe any significant change in the absorption spectrum when PVP of low molecular weight was used, indicating that particle sizes remain similar.

As discussed earlier, evolution of CO_2 gas was also observed during the reduction of silver ions in the presence of PVP. CO_2 gas was measured under identical experimental conditions to see if there exists any correlation between the concentration of evolved gas and the growth of the silver plasmon absorption band. In the presence of PVP, the amount of CO_2 evolved was measured to be 1.44 μmol after 28 h. It may be noted that the amount of CO_2 evolved in the absence of PVP was higher after an identical time period. This is because the rate of reduction and aggregation is much slower in the presence of PVP than in its absence in formamide. However, it cannot be quantified in terms of amount of CO_2 evolved per mol of silver metal formed, as some Ag^+ ions always remain unreduced in formamide containing PVP.

The bulk measurements can provide some evidence about the size of the nanoparticles, but they do not provide exact information about the particle size and shape. Atomic force or electron microscopy is an effective method to provide surface topography and phase images. For nanoparticles prepared in the presence of stabilizers, TEM was used. A typical TEM image for a solution containing 1% PVP (wt/v) is shown in Figure 6. The average size of the particles in the presence of 1% PVP was found to be 25 nm (Figure 6a). At certain places, twinning was also observed, a phenomenon common for fcc structures and which is clear from the diffraction pattern (Figure 6b). It is important to mention that the samples for TEM were prepared by putting a drop of the silver sol over the carbon-supported copper grid and were dried at room temperature. As formamide is highly viscous and has a high boiling point, it took a lot of time to dry the samples. TEM studies (Figure 6c) revealed that in the drying process the silver film formation also took place encompassing many particles, having particular shapes (disk type). Due to the formation of such crystals at certain places, it becomes difficult to comment on the variation in the size of the particles with time.

The morphology of the silver nanoparticles without any stabilizer was probed using AFM. For this, glass slides were suspended in the solution for a certain period of time (24 h). After the film formation, the slides were taken out and dried in air before being examined under AFM. Figure 7 shows that the particles were around 100 nm in size having spherical shape. The glass plates (slides) prepared by the above method showed time-dependent optical properties on the packing density of

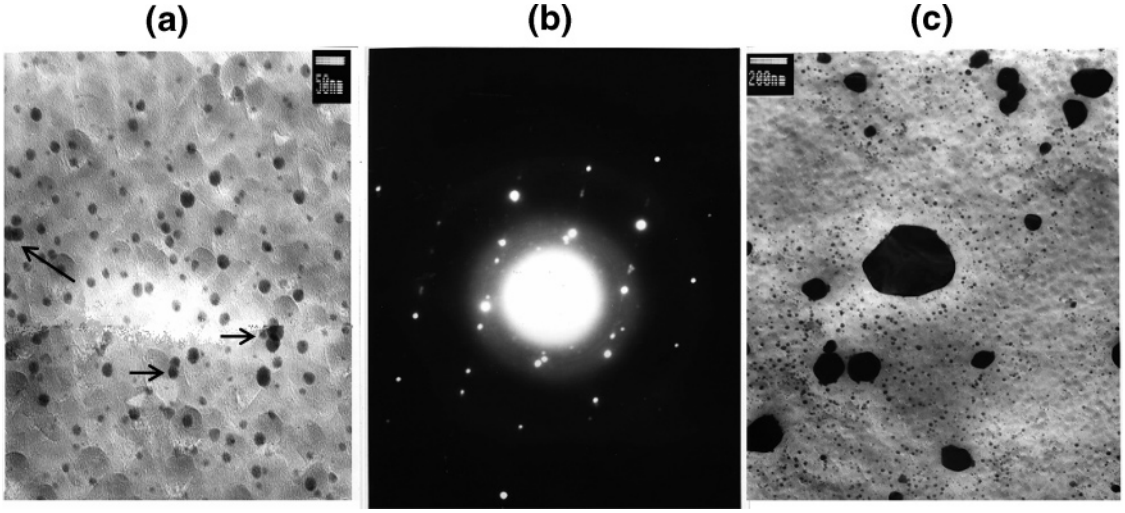

Figure 6. Transmission electron micrograph of silver nanoparticles in formamide (a) for 5×10^{-3} mol dm^{-3} silver ions concentration containing 1% PVP (wt/v) [showing twinning of particles]; (b) electron diffraction pattern from a twin particle; and (c) large flat particles with definite geometric shapes.

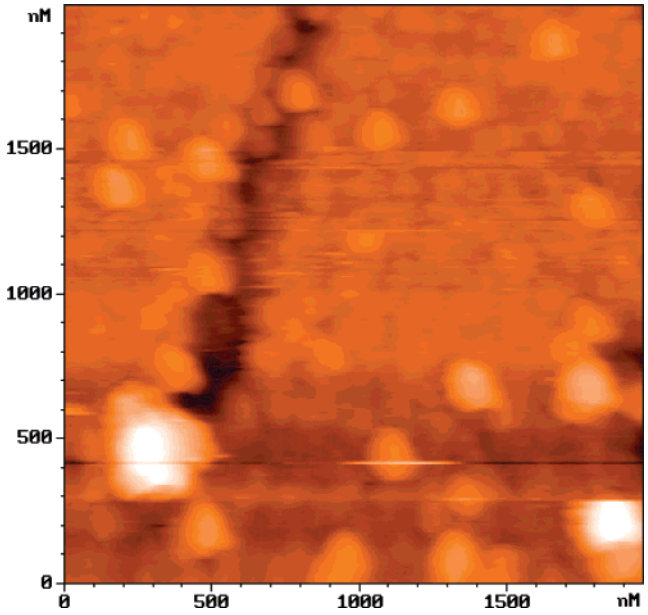

Figure 7. AFM image of silver nanoparticles prepared by reduction of 5×10^{-3} mol dm^{-3} silver ions in neat formamide at room temperature.

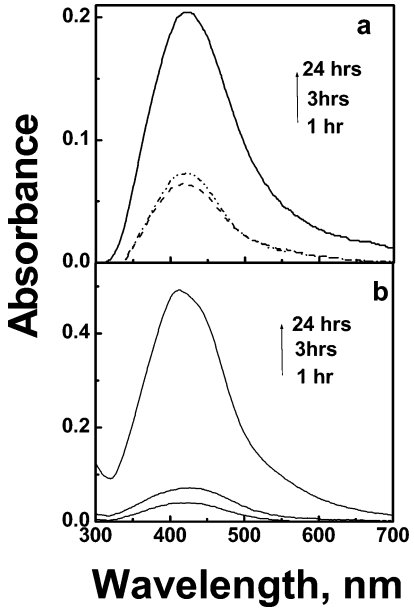

Figure 8. Time-dependent UV−visible absorption spectra of silver nanoparticles after dispersing in (a) formamide and (b) methanol.

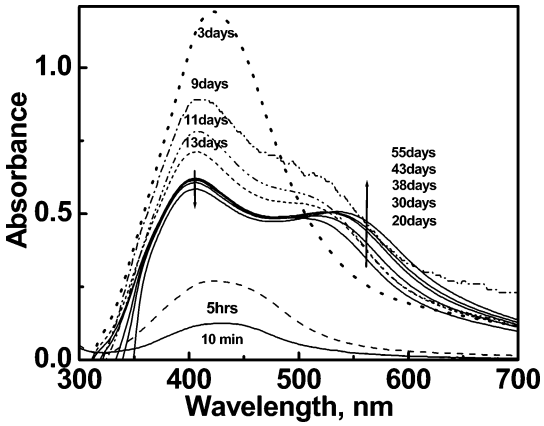

Figure 9. Time-dependent UV−visible absorption spectra of silver nanoparticles after dispersing in methanol showing conversion of nanospheres to polygonal shaped particles.

silver particles. This is similar to that as predicted by the Maxwell−Garnett theory and as demonstrated by Ung et al.[40] It is important to mention here that films prepared in the presence and absence of light showed similar results.

To confirm that the above-mentioned results are not due to photolytic reaction of NO_3^-, few experiments were also repeated with silver perchlorate. No significant difference with silver perchlorate was observed.

There is a possibility of the generation of oxidizing species during reduction of silver ions by formamide. Methanol is known to be an efficient scavenger of oxidizing species. Therefore, to confirm that during reduction of Ag^+ in formamide oxidizing radicals are produced, the following experiments were carried out. The reduction of silver ions was initiated in neat formamide before addition of methanol. At a noted time (1 h), methanol was added to the silver dispersion in formamide such that the formamide:methanol ratio was 1:5. To see the effect of methanol, a control experiment was also done by adding the same volume of neat formamide to the silver dispersion at an identical time. After dilution, the absorption spectra of silver nanoparticles were monitored for various time periods. The results are shown in Figure 8. It can be seen that the dispersion diluted with methanol (Figure 8a) showed higher absorbance as compared to that diluted with formamide (Figure 8b) in an identical time period. In the dispersion containing methanol, the larger increase in the absorbance of Ag nanoparticles is due to scavenging of oxidizing species generated during the reduction of silver ions. In addition, methanol radicals produced by scavenging oxidizing radicals also have reducing properties. The combined effect of the above-mentioned processes led to the increase in the rate of reduction, and hence the absorbance due to surface plasmon absorption band of Ag nanoparticles increased. Dispersion of formamide containing methanol was monitored for almost 2 months, and the results are shown in Figure 9. It can be noticed from the figure that after 20 days there was no significant decrease in the absorption intensity at 400 nm. However, the intensity of the particles, showing maxima at 550 nm, continued to increase. The growth of the absorption band showing maximum at around 550 nm and concomitant decrease of the band showing maximum at 400 nm shows conversion of spherical shaped particles to rectangular shaped particles.[41] It is pertinent to mention here that spectra in Figures 8a and 9 are broader and red shifted as compared to those of Ag colloids made in neat alcohols,[42,43] suggesting that the particle size is bigger. This is due to the fact that the rate of reduction of Ag^+ ions is lower in the formamide−methanol mixture as the potential of methanolic radicals is lower than hydrated electron[42] and isopropyl radicals.[43] Recently, using theoretical calculations, Tojo et al.[37] have suggested that for the formation of small nanoparticles instant seed nucleation is required. This could be the reason for observing a broader surface plasmon absorption band as well as larger particles in the present case.

A distinct smell of ammonia was noticed in the formamide and methanol mixture. This shows that methanol also forms a complex with formamide in addition to scavenging oxidizing species. This complex in turn undergoes some chemical reaction, and during this process the reduction of silver ions also takes place. Recently, using theoretical calculations it has been shown that addition of methanol to formamide changes the relative ability of the carbonyl against the amide group for hydrogen bonding with methanol.[31,32] It has been calculated that bonding by the amide group is more energetically feasible than binding

by the carbonyl group. Thus, there exists a possibility that, due to the change in the structure of formamide in the presence of methanol, the reaction path for the dissociation and/or oxidation of formamide changes, which in turn affects the agglomeration of the nanoparticles.

Reaction of the Silver Nanoparticles with $CHCl_3$ and Toluene in the Presence of Oxygen. To find the possibility of the silver nanoparticles reacting with chloroform, particles were prepared in formamide containing 1% PVP, which was diluted 4 times with chloroform. The solution was vigorously shaken for 30 min. On standing, the color of the silver sol gradually faded due to oxidation in the formamide layer. The results corroborate the findings reported in aqueous solution;[35] however, in N_2-bubbled solution the oxidation of particles was very slow. This shows that electron transfer from silver particles is facilitated in the presence of oxygen. A similar observation was made when toluene was added to silver dispersions.

The reaction of silver nanoparticles with $CHCl_3$ is indicative of the strong reducing power of the particles. As the nanoparticles have more surface atoms, the unsaturation at the surface is very high. In the presence of an organic molecule, which is an electrophile, the surface atom acquires an excess positive charge and the rest of the nanoparticles a corresponding negative charge. In the presence of oxygen, this excess negative charge is removed and the oxidation of the silver particles can proceed. This could be the reason for observing fast oxidation of silver particles in an aerated solution as compared to that in a N_2-bubbled solution.

Similarly, the reactivity of silver nanoparticles with toluene was investigated. After addition of toluene to a silver dispersion in formamide, the solution was vigorously shaken for 30 min. On standing, the color of the silver sol gradually faded due to oxidation in the formamide layer. However, in a N_2-bubbled solution, the oxidation of particles was very slow. It is known that oxidation of toluene leads to the formation of benzaldehyde.[44,45] As metal particles can act as a sink for electrons, it appears that in the presence of silver particles, there is a possibility of oxidation of toluene, which is facilitated by the presence of oxygen.

Surface Modification Studies. To further confirm the above observations, we have carried out surface modification studies of silver films in the presence of Na_4EDTA. Silver film deposition was carried out as explained earlier. In the absence of any complexing agent, films were quite stable, and we could not see any significant change in the absorption of silver films. However, when a slide of silver film was dipped in the solution of Na_4EDTA, the color of the film changed from brown to pink due to adsorption of Na_4EDTA on the silver film. Figure 10 shows the effect of Na_4EDTA on the surface plasmon absorption band of silver film. The observed change in the intensity and surface plasmon absorption band is due to the disturbance at the surface of the electron gas. In the presence of oxygen, the oxidation of silver film takes place. This shows that the reduction potential of Ag particles is affected in the presence of Na_4EDTA[46] and becomes more negative than the $O_2/O_2^{-\bullet}$ couple, -0.33 V vs NHE.[47] To see whether electron transfer from silver film to MV^{2+} takes place in the presence of Na_4EDTA, a glass slide of silver particles complexed with Na_4EDTA was dipped in a N_2-bubbled aqueous solution containing methyl viologen (MV^{2+}). No significant change in the color of the slide as well as no sign of the formation of $MV^{+\bullet}$ radical was observed. Thus, it appears that the reduction potential of Ag particles in the presence of Na_4EDTA lies below that of the $MV^{2+}/MV^{+\bullet}$ couple, -0.446 V (vs NHE).[47] It is important to mention here

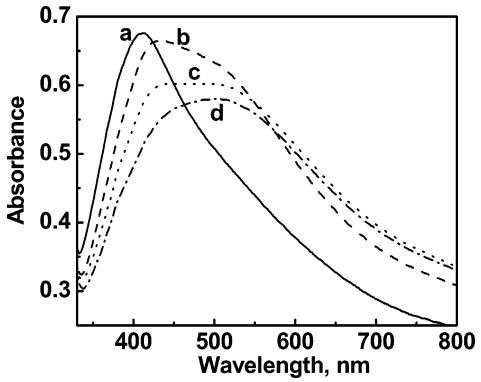

Figure 10. Time-dependent UV−visible absorption spectra of (a) silver film obtained by reduction of 1×10^{-2} mol dm^{-3} silver ions in formamide; after dipping the film in an aqueous solution of 5×10^{-2} mol dm^{-3} Na_4EDTA for (b) 30 min, (c) 70 min, and (d) 200 min.

that the stability of the film under inert conditions enhanced drastically as compared to when it was exposed to air. The above results show that Fermi level of Ag particles becomes more negative in the presence of Na_4EDTA, and it seems to lie between -0.33 and -0.446 V vs NHE.

Conclusion

We have demonstrated the synthesis of silver nanoparticles in formamide at room temperature without adding any reductant from outside. In the presence of a proper stabilizer, nanoparticles of silver metal can be stabilized. Surface-modified particles (or films) show optical properties significantly different from those of the primary silver dispersion (or film). The silver nanoparticles also act as redox catalysts due to the shift in the Fermi level toward more negative potential. Moreover, the method described here presents a simple approach for the formation of silver nanoparticles.

References and Notes

(1) Faraday, M. *Philos. Trans. R. Soc. London* **1857**, *147*, 145.
(2) Hirai, H.; Nakao, Y.; Toshima, N. *Chem. Lett.* **1978**, 545.
(3) (a) Henglein, A. *Chem. Rev.* **1989**, *89*, 1861. (b) Kamat, P. V. *Chem. Rev.* **1993**, *93*, 267.
(4) Belloni, J. *Radiat. Res.* **1998**, *150*, 39.
(5) Henglein, A.; Meisel, D. *J. Phys. Chem. B* **1998**, *102*, 8386.
(6) Dimitrijevic, N. M.; Bartels, D. M.; Jonah C. D.; Takahashi, K.; Rajh, T. *J. Phys. Chem. B* **2001**, *105*, 954.
(7) Marignier, J. L.; Belloni, J.; Delcourt, M. V.; Chevalier, J. P. *Nature* **1985**, *317*, 344.
(8) Cointet, C. de; Mostafavi, M.; Khatouri, J.; Belloni, J. *J. Phys. Chem. B* **1997**, *101*, 3512.
(9) Kapoor, S. *Langmuir* **1998**, *14*, 1021.
(10) Kapoor, S. *Langmuir* **1999**, *15*, 4365.
(11) Kapoor, S. *Langmuir* **2000**, *16*, 5496.
(12) Ahmadi, T. S.; Wang, Z. L.; Green, T. C.; Henglein, A.; El-Sayed, M. A. *Science* **1996**, *272*, 1924.
(13) Ershov, B. G.; Henglein, A. *J. Phys. Chem.* **1998**, *102*, 10663, 10667.
(14) Templeton, A. C.; Wuelfing, W. P.; Murray, R. W. *Acc. Chem. Res.* **2000**, *33*, 27.
(15) Storhoff, J. J.; Mirkin, C. A. *Chem. Rev.* **2000**, *100*, 409.
(16) Shipway, A. N.; Katz, E.; Willner, I. *ChemPhysChem* **2000**, *1*, 18.
(17) Zhong, C. J.; Maye, M. M. *Adv. Mater.* **2001**, *13*, 1507.
(18) Henglien, A. *Isr. J. Chem.* **1993**, *33*, 77.
(19) Bruchez, M.; Moronne, M.; Gin, P.; Weiss, S.; Alivisatos, A. P. *Science* **1998**, *281*, 2013.
(20) Brust, M.; Bethell, D.; Keily, C. J.; Shiffrin, D. J. *Langmuir* **1998**, *14*, 5425.
(21) Geirsig, M.; Pastoriza-Santos, I.; Liz-Marzan, L. M. *J. Mater. Chem.* **2004**, *14*, 607.
(22) Link, S.; El-Sayed, M. A. *J. Phys. Chem. B* **1999**, *103*, 8410.
(23) Musick, M. D.; Pena, D. J.; Botsko, S. L.; McEvoy, T. M.; Richardson, T. N.; Natan, M. J. *Langmuir* **1999**, *15*, 844.

(24) Pastoriza-Santos, I.; Liz-Marzan, L. M. *Langmuir* **1999**, *15*, 948.
(25) Pastoriza-Santos, I.; Liz-Marzan, L. M. *Pure Appl. Chem.* **2000**, *72*, 83.
(26) Pastoriza-Santos, I.; Serra-Rodriguez, C.; Liz-Marzan, L. M. *J. Colloid Interface Sci.* **2000**, *221*, 236.
(27) Pastoriza-Santos, I.; Liz-Marzan, L. M. *Langmuir* **2000**, *18*, 2888.
(28) Pastoriza-Santos, I.; Liz-Marzan, L. M. *Nano Lett.* **2002**, *2*, 903.
(29) Han, M. Y.; Quek, C. H. *Langmuir* **2000**, *16*, 362
(30) Han, M. Y.; Quek, C. H.; Huang, W.; Chew, C. H.; Gan, L. M. *Chem. Mater.* **1999**, *11*, 1144.
(31) Fu, A.-P.; Du, D.-M.; Zhou, Z.-Y. *Chem. Phys. Lett.* **2003**, *377*, 537.
(32) Ojha, A. K.; Srivastava, S. K.; Koster, J.; Shukla, M. K.; Leszczynski, J.; Asthana, B. P.; Kiefer, W. *J. Mol. Struct.* **2004**, *689*, 127.
(33) Hoffman, M. R.; Martin, S. T.; Choi, W.; Bahnemann, D. W. *Chem. Rev.* **1995**, *95*, 69.
(34) Linsebigler, A. L.; Lu, G.; Yates, J. T. *Chem. Rev.* **1995**, *95*, 735.
(35) (a) Henglein, A.; Linnert, T.; Mulvaney, P. *Ber. Bunsen-Ges. Phys. Chem.* **1990**, *94*, 1449. (b) Henglein, A.; Mulvaney, P.; Linnert, T. *Electrochim. Acta* **1991**, *36*, 1743.
(36) Yu, J. Y.; Schreiner, S.; Vaska, L. *Inorg. Chim. Acta* **1990**, *170*, 145.
(37) Tojo, T.; Blanco, M. C.; Rivadulla F.; Lopez-Quintela, M. M. *Langmuir* **1997**, *13*, 1970.
(38) Lawless, D.; Kapoor, S.; Kennepohl, P.; Meisel, D.; Serponne, N. *J. Phys. Chem.* **1994**, *98*, 9619.
(39) Li, T.; Moen, J.; Morrone, A. A.; Mecholsky, J. J.; Talham, D. R.; Adair, J. H. *Langmuir* **1999**, *15*, 4328.
(40) Ung, T.; Liz-Marzan, L. M.; Mulvaney, P. *Colloids Surf., A* **2000**, *202*, 119.
(41) Mock, J. J.; Barbic, M.; Smith, D. R.; Schultz, D. A.; Schultz, S. *J. Chem. Phys.* **2002**, *116*, 6755.
(42) Mostafavi, M.; Dey, G. R.; Francois, L.; Belloni, J. *J. Phys. Chem. A* **2002**, *106*, 10184.
(43) Huang, Z.-Y.; Mills, G.; Hajek, B. *J. Phys. Chem.* **1993**, *97*, 11542.
(44) Fuerte, A.; Hemandez-Alonso, M. D.; Maira, A. J.; Martinez-Arias, A.; Fernandez-Garcia, M.; Conesa, J. C.; Soria, J.; Munuera, G. *J. Catal.* **2002**, *212*, 1.
(45) Fuerte, A.; Hemández-Alonso, M. D.; Maira, A. J.; Martinez-Arias, A.; Fernández-Garcia, M.; Conesa, J. C.; Soria, J. *Chem. Commun.* **2001**, 2178.
(46) Remita, S.; Mostafavi, M.; Delcourt, M. O. *J. Phys. Chem.* **1996**, *100*, 10187.
(47) Wardman, P. *J. Phys. Chem. Ref. Data* **1989**, *18*, 1637.